Effects of extracellular potassium diffusion on electrically coupled neuron networks

Xing-Xing Wu
Department of Physics, Xiamen University, Xiamen 361005, P. R. China

Jianwei Shuai*
Department of Physics, State Key Lab of Cellular Stress Biology, Innovation Center for Cell Signaling Network, and Fujian Provincial Key Laboratory of Theoretical and Computational Chemistry, Xiamen University; Xiamen 361005, P. R. China

(Received 31 July 2014; published 23 February 2015)

Potassium accumulation and diffusion during neuronal epileptiform activity have been observed experimentally, and potassium lateral diffusion has been suggested to play an important role in nonsynaptic neuron networks. We adopt a hippocampal CA1 pyramidal neuron network in a zero-calcium condition to better understand the influence of extracellular potassium dynamics on the stimulus-induced activity. The potassium concentration in the interstitial space for each neuron is regulated by potassium currents, Na^+-K^+ pumps, glial buffering, and ion diffusion. In addition to potassium diffusion, nearby neurons are also coupled through gap junctions. Our results reveal that the latency of the first spike responding to stimulus monotonically decreases with increasing gap-junction conductance but is insensitive to potassium diffusive coupling. The duration of network oscillations shows a bell-like shape with increasing potassium diffusive coupling at weak gap-junction coupling. For modest electrical coupling, there is an optimal K^+ diffusion strength, at which the flow of potassium ions among the network neurons appropriately modulates interstitial potassium concentrations in a degree that provides the most favorable environment for the generation and continuance of the action potential waves in the network.

DOI: 10.1103/PhysRevE.91.022712 PACS number(s): 87.19.lj, 05.45.Xt

I. INTRODUCTION

Neurons are excitable cells. During neural activity, potassium ions are released, and the increased extracellular potassium concentration in turn alters neuronal excitability. It has been proposed that the extracellular potassium concentration plays an important role in some abnormal functions, such as hypoxia-induced spreading depression [1], diabetes, and arrhythmias [2–4].

The extracellular potassium accumulation during neuronal firing was observed by Frankenhaeuser and Hodgkin in 1956 [5]. It has been suggested that a direct application of a high potassium solution could induce hippocampal epileptic activity [6], and epileptiform burst discharges could exhibit different patterns due to the variation of background extracellular potassium concentrations [7,8]. Epilepsy has also been shown to be connected with a reduction of the Na^+-K^+ pump [9] and impairment of the glial K^+ uptake [10]. It has been shown that low-calcium epileptiform activity was associated with the diffusion of potassium ions [11,12] and that the elevation of extracellular potassium modulated cortical oscillatory activities [13]. However, it was argued that the potassium accumulation was only an influential factor in the course of neuronal firing but could not initiate seizure activity [14,15].

Modeling studies pointed out the critical roles of extracellular potassium in modulating neuron dynamics [16]. It has also been shown that changes in the interstitial potassium concentration ($[K^+]_o$) modulated the frequency of bursting in a single-neuron model [17,18]. A two-compartment cortical neuron model with extracellular potassium concentration exhibited bi-stability with hysteresis between tonic firing and bursting [19]. Moreover, the potassium homeostasis appeared to be a necessary mechanism for neurons to function properly [20–22].

In many computational studies, communication among neurons involves chemical and electrical synapses [23–26] and other nonsynaptic mechanisms. Lateral diffusion of K^+ has been suggested as one nonsynaptic interaction between neurons and has gained increasing attention [17,27–30]. In the CA1 region of the mammalian hippocampus, neurons are densely packed, thereby creating favorable conditions for potassium lateral diffusion coupling. It has been suggested that, in a network of zero-Ca^{2+} CA1 pyramidal neurons, potassium lateral diffusion coupling is involved in inducing and sustaining neuronal activity [31,32] and synchronizing neuronal firing [33], for which it has been assumed that nearby neurons have only one type of interaction, which is provided by potassium lateral diffusion.

In addition, in the CA1 region of the hippocampus, electrical coupling by gap junctions has been shown to play an important role in oscillatory network activity [34–37]. But this type of coupling is usually absent in the studies of potassium coupling. In this paper we present a neuron network model where hippocampal CA1 pyramidal neurons are coupled through gap junctions and potassium diffusion. Electrical coupling is included and expressed as somatic contacts between nearby neurons. The chemical synaptic transmission and calcium and Ca^{2+}-activated currents are omitted in the condition of zero extracellular calcium. Because chemical synapses are not incorporated in the system, whether the neurons are excitatory or inhibitory is not important.

The contents of this paper are given as follows. In Sec. II we present the equations describing each neuron of the network and the couplings between neighboring cells. Then in Sec. III we make comparisons of the response of the electrically

*jianweishuai@xmu.edu.cn

coupled network to external stimulation with and without potassium lateral diffusion. Later, by varying the values of potassium coupling strength and gap-junction conductance, an interesting result observed is that the relation of the duration of network oscillations to potassium coupling strength is nonmonotonic at medium gap-junction conductance. Finally, conclusions are made in Sec. IV.

II. FORMALISM

A schematic of our model is shown in Fig. 1. The neuron network in our simulations has 50×50 identical cells [Fig. 1(d)]. For each cell, we adopt a 16-compartment hippocampal CA1 pyramidal neuron model with one soma compartment and other compartments for apical dendrites and basal dendrites [Fig. 1(a)] [38]. For potassium accumulation, the variable $[K^+]_o$ represents potassium concentration of the interstitial space around soma. Potassium accumulates more intensively in somatic layers than in dendritic layers [12,15], and the transient changes in extracellular potassium concentrations have a greater effect over neuronal behavior than the changes in the intracellular sodium concentrations [21]. Therefore, only somatic potassium accumulation is incorporated in this neuron model.

These cells are connected through gap junctions and potassium diffusion [Fig. 1(b)]. The electrical coupling connects nearest neighboring cells with gap-junction conductance g_{gap}, while K^+ diffuses between nearest neighboring cells and between second nearest neighboring cells [Fig. 1(c)].

The values and meaning of model parameters are given in Table I. All conductance measurements are corrected for the specific area of each compartment and are expressed in the unit of mS/cm^2. Each dendrite compartment has a diameter of 5.2 μm and length of 81.7 μm, giving an area of 1334.67 μm^2. The soma has an approximate area of 1000 μm^2 [38]. Hence, the value of soma axial conductance ($g_{5,4}$, $g_{5,6}$) is larger than the value of dendrite axial conductance between soma and dendrite ($g_{4,5}$, $g_{6,5}$).

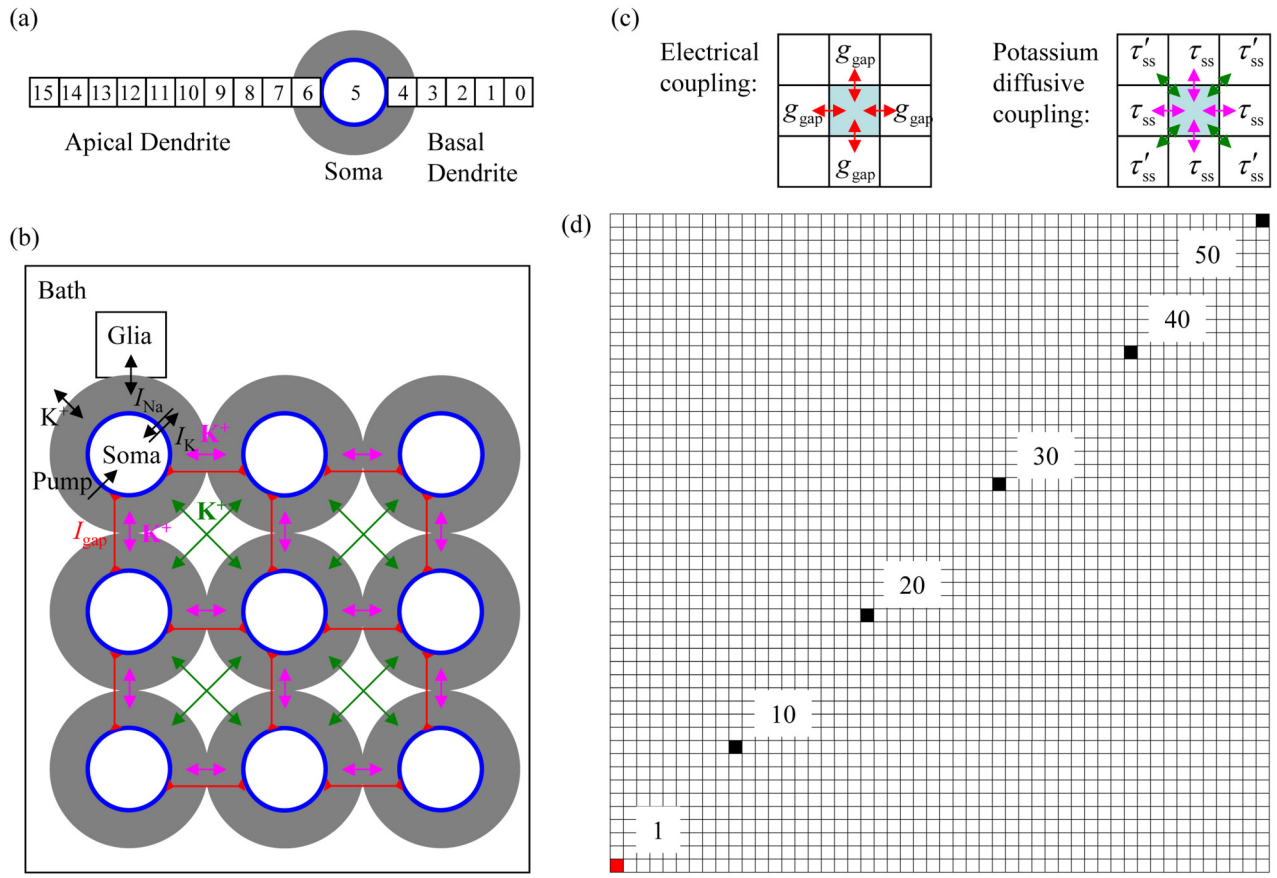

FIG. 1. (Color online) (a) Structure of a CA1 pyramidal neuron. Sixteen compartments represent for dendrites and one compartment for soma. The soma (blue circle) is surrounded by an interstitial space (gray area) where K^+ may accumulate. (b) A network of 3×3 neurons is used to illustrate mechanisms for regulating interstitial potassium and how neurons are coupled. When one neuron is stimulated, potassium ions are released into the interstitial space through potassium channels. The Na^+-K^+ pump and glia remove excessive K^+. The concentration gradient of K^+ tends to move them into the bath and interstitial spaces of other neighboring cells. The lateral diffusion occurs between nearest neighbors (pink lines with arrowheads) and second nearest neighbors (green lines with arrowheads). Besides potassium coupling, electrical coupling is through gap junctions (red lines with triangles). (c) This network is further simplified by replacing each neuron with a square to indicate values of gap-junction conductance and lateral diffusion time constant between neighboring cells. (d) Structure of 50×50 neurons for the following simulations unless otherwise specified. Electrical stimuli are applied to cell 1 (red square).

TABLE I. Parameter values. Sources: (a) Ref. [38]; (b) definition; (c) estimated and/or modified values; (d) Ref. [31]; (e) Ref. [33].

Symbol	Parameter	Value	Source
R	Radius of soma	8.9×10^{-4} cm	(a)
A	Area of soma	$4\pi R^2$	(b)
$\text{Volume}_{\text{cell}}$	Volume of soma	$4\pi R^3/3$	(b)
$\text{Volume}_{\text{shell}}$	Volume of the interstitial space around soma	$4\pi R^3 r_{\text{V}}/3$	(b)
r_{V}	$r_{\text{V}} = \frac{\text{Volume}_{\text{shell}}}{\text{Volume}_{\text{cell}}}$	0.15	(d)
F	Faraday's constant	96485 C/mol	(b)
τ_{bs}	Diffusion time constant	412 ms	(c)
κ	Potassium coupling strength	0–1.7	(c)
τ_{ss}	Lateral diffusion time constant between nearest cells	$\frac{1000\,\text{ms}}{10^{\kappa}-1}$ ms	(b)
$\tau_{\text{ss}}^{'}$	Lateral diffusion time constant between second nearest cells	$3.3\tau_{\text{ss}}$	(c)
C_{s}	Soma capacitance	1.0 μF/cm^2	(d)
g_{NaF}	Fast Na^+ conductance	20.5 mS/cm^2	(e)
g_{NaP}	Persistent Na^+ conductance	0.24 mS/cm^2	(d)
g_{KDR}	Delayed-rectifier K^+ conductance	19.7 mS/cm^2	(e)
g_{KA}	A-type transient K^+ conductance	3.0 mS/cm^2	(d)
g_{KM}	Muscarinic K^+ conductance	3.0 mS/cm^2	(d)
g_{sLeak}	Soma leakage conductance	1.8 mS/cm^2	(d)
$g_{5,4}$,$g_{5,6}$	Soma axial conductance	7.35 mS/cm^2	(a, c)
g_{gap}	Gap junction conductance	0.275–0.7 mS/cm^2	(c)
E_{Na}	Sodium reversal potential	67.0 mV	(d)
E_{sLeak}	Soma leakage reversal potential	−54.4 mV	(c)
I_{max}	Pump maximal current	24.0 μA/cm^2	(c)
$[K^+]_{\text{bath}}$	Potassium concentration in the bath	7.6 mM	(e)
$[K^+]_{\text{eq}}$	Equilibrium potassium concentration	$[K^+]_{\text{bath}}$	(e)
$[B]_{\text{max}}$	Maximal buffer capacity	265 mM	(d)
r_{b}	Backward rate of buffer mechanism	0.0008 ms^{-1}	(d)
r_{f0}	Equilibrium forward rate of buffer mechanism	0.0008 mM^{-1}/ms	(d)
$[K^+]_{\text{th}}$	Threshold $[K^+]_{\text{o}}$ for glia buffer	15 mM	(d)
C_{d}	Dendrite capacitance	1.88 μF/cm^2	(d)
$g_{4,5}$,$g_{6,5}$	Dendrite axial conductance between soma and dendrite	5.51 mS/cm^2	(a, c)
$g_{n\pm1,n}$	Dendrite axial conductance between dendritic compartments (n, $n \pm 1 \neq 5$)	3.67 mS/cm^2	(d)
g_{dLeak}	Dendrite leakage conductance	0.0292 mS/cm^2	(d)
E_{dLeak}	Dendrite leakage reversal potential	−54.4 mV	(c)

A. Membrane potential dynamics

The ordinary differential equations governing the membrane potential are as follows:

$$C_{\text{s}}\frac{dV_{\text{s}}}{dt} = -(I_{\text{Na}} + I_{\text{K}} + I_{\text{sLeak}} + I_{\text{pump}} + I_{\text{sd}}) + I_{\text{stim}}, \quad (1)$$

$$C_{\text{d}}\frac{dV_{\text{d},n}}{dt} = -(I_{\text{dLeak},n} + I_{\text{dd},n}), \quad (2)$$

where $0 \leqslant n \leqslant 15$ and $n \neq 5$. V_{s} is the membrane potential for the somatic compartment and $V_{\text{d,n}}$ for other dendritic compartments. The stimulus current I_{stim} is applied to the soma.

The relevant somatic currents include two active Na^+ currents ($I_{\text{Na}} = I_{\text{NaF}} + I_{\text{NaP}}$), three active K^+ currents ($I_{\text{K}} = I_{\text{KDR}} + I_{\text{KA}} + I_{\text{KM}}$), the passive current I_{sLeak}, the current caused by the Na^+-K^+ pump I_{pump} and the axial current I_{sd}, which are given by

$$\begin{aligned}
I_{\text{NaF}} &= g_{\text{NaF}} m^3 h (V_{\text{s}} - E_{\text{Na}}),\\
I_{\text{NaP}} &= g_{\text{NaP}} w (V_{\text{s}} - E_{\text{Na}}),\\
I_{\text{KDR}} &= g_{\text{KDR}} n^4 (V_{\text{s}} - E_{\text{K}}),\\
I_{\text{KA}} &= g_{\text{KA}} ab (V_{\text{s}} - E_{\text{K}}),\\
I_{\text{KM}} &= g_{\text{KM}} u^2 (V_{\text{s}} - E_{\text{K}}),\\
I_{\text{sLeak}} &= g_{\text{sLeak}} (V_{\text{s}} - E_{\text{sLeak}}),\\
I_{\text{pump}} &= I_{\text{max}}/[1 + ([K^+]_{\text{eq}}/[K^+]_{\text{o}})]^2,\\
I_{\text{sd}} &= g_{5,4}(V_{\text{s}} - V_4) + g_{5,6}(V_{\text{s}} - V_6),
\end{aligned} \quad (3)$$

where $E_{\text{K}} = 26.71 \times \ln(\frac{[K^+]_{\text{o}}}{140})$ mV. The reason that the Na^+-K^+ pump is electrogenic is that more sodium is extruded than potassium absorbed.

TABLE II. Kinetics for gating variables [31].

Ordinary differential equation for gating variable
$\frac{dm}{dt} = \frac{11.7\times(11.5-V_s)}{\exp\left(\frac{11.5-V_s}{13.7}\right)-1.0}(1.0-m) - \frac{0.4\times(V_s-10.5)}{\exp\left(\frac{V_s-10.5}{4.2}\right)-1.0}m$
$\frac{dh}{dt} = \frac{0.67}{\exp\left(\frac{V_s+50.0}{5.5}\right)}(1.0-h) - \frac{2.24}{\exp\left(\frac{72.0-V_s}{29.0}\right)+1.0}h$
$\frac{dw}{dt} = \frac{\frac{0.07}{\exp\left(\frac{-V_s-50.0}{2.0}\right)+1.0}-w}{0.2}$
$\frac{dn}{dt} = \frac{0.00049\times V_s}{1.0-\exp\left(\frac{-V_s}{25.0}\right)}(1.0-n) - \frac{0.00008\times(V_s-10.0)}{\exp\left(\frac{V_s-10.0}{10.0}\right)-1.0}n$
$\frac{da}{dt} = \frac{0.0224\times(V_s+30.0)}{1.0-\exp\left(\frac{-V_s-30.0}{15.0}\right)}(1.0-a) - \frac{0.056\times(V_s+9.0)}{\exp\left(\frac{V_s+9.0}{8.0}\right)-1.0}a$
$\frac{db}{dt} = \frac{0.0125}{\exp\left(\frac{V_s+8.0}{14.5}\right)}(1.0-b) - \frac{0.094}{\exp\left(\frac{-V_s-63.0}{16.0}\right)+1.0}b$
$\frac{du}{dt} = 0.0084\times\exp\left(\frac{V_s+26.0}{40.0}\right)(1.0-u) - \frac{0.0084}{\exp\left(\frac{V_s+26.0}{61.0}\right)}u$

The currents through the voltage-dependent channels are controlled by the gating variables m, h, w, n, a, b, and u. They obey the form

$$\frac{dx}{dt} = \frac{x_\infty(V)-x}{\tau_x} = \alpha_x(V) - x[\alpha_x(V)+\beta_x(V)], \tag{4}$$

where x represents m, h, w, n, a, b, and u. Table II gives the details of the equations for each gating variable.

For dendrite compartments, there are two passive currents given by

$$\begin{aligned} I_{\mathrm{dLeak},n} &= g_{\mathrm{dLeak}}(V_{d,n} - E_{\mathrm{dLeak}}),\\ I_{\mathrm{dd},n} &= g_{n,n-1}(V_{\mathrm{d},n} - V_{n-1}) + g_{n,n+1}(V_{\mathrm{d},n} - V_{n+1}), \end{aligned} \tag{5}$$

where $I_{\mathrm{dd,n}}$ is the axial current caused by the potential difference between neighboring dendrite sections. Compartments 0 and 15 have only one neighboring compartment contributing to the axial current.

B. Potassium dynamics and coupling

The outside space of the soma consists of an interstitial space and the bath. The potassium concentration in the bath is always constant, while the interstitial potassium concentration can elevate from its resting value caused by the K^+ release from the cytoplasm. The interstitial potassium concentration $[K^+]_o$ depends on

$$\frac{d[K^+]_o}{dt} = J_{\mathrm{currents}} - J_{\mathrm{pump}} + J_{\mathrm{glia}} - J_{\mathrm{bath}} \tag{6}$$

with each potassium flux given by

$$\begin{aligned} J_{\mathrm{currents}} &= \frac{I_K \times A \times 10^{-3}}{F \times \mathrm{Volume}_{\mathrm{shell}}},\\ J_{\mathrm{pump}} &= \frac{2 \times I_{\mathrm{pump}} \times A \times 10^{-3}}{F \times \mathrm{Volume}_{\mathrm{shell}}},\\ J_{\mathrm{glia}} &= r_b \times ([B]_{\max} - [B]) - r_f \times [K^+]_o \times [B],\\ J_{\mathrm{bath}} &= \frac{([K^+]_o - [K^+]_{\mathrm{bath}})}{\tau_{\mathrm{bs}}}. \end{aligned} \tag{7}$$

A phenomenological model was used to simulate the glial potassium uptake system that controls the potassium accumulation in the interstitial volume [20]. We adopt this buffering scheme, which is given by

$$\frac{d[B]}{dt} = r_b \times ([B]_{\max} - [B]) - r_f \times [K^+]_o \times [B], \tag{8}$$

where

$$r_f = \frac{r_{f0}}{1+\exp\left(\frac{[K^+]_o-[K^+]_{\mathrm{th}}}{-1.15}\right)}. \tag{9}$$

There are only two types of couplings in our model, i.e., the electrical coupling and the potassium diffusive coupling. Because the neurons are modeled in zero-calcium conditions, chemical synapses are neglected. Figure 1(b) gives a schematic diagram of the couplings between cells. As we can see, two nearest cells are connected through both gap junctions (red lines with triangles) and potassium diffusion (pink lines with arrowheads). Moreover, potassium ions diffuse between two second nearest cells (green lines with arrowheads).

To model potassium coupling between neighbor cells, a new item is added to the right side of Eq. (6) for interstitial potassium dynamics for a cell numbered i:

$$\begin{aligned} \frac{d[K^+]_o^i}{dt} &= J^i_{\mathrm{currents}} - J^i_{\mathrm{pump}} + J^i_{\mathrm{glia}} - J^i_{\mathrm{bath}} - J^i_{\mathrm{shell}},\\ J^i_{\mathrm{shell}} &= \sum_j \frac{([K^+]^i_o - [K^+]^j_o)}{\tau_{\mathrm{ss}}} + \sum_k \frac{([K^+]^i_o - [K^+]^k_o)}{\tau'_{\mathrm{ss}}}, \end{aligned} \tag{10}$$

where τ_{ss} and τ'_{ss} is the diffusion time constant between interstitial spaces of nearest cells and between interstitial spaces of second nearest cells, respectively. As described by Eq. (10), the potassium flux J^i_{shell} is the sum of the K^+ fluxes between the given cell and its nearest cells and between the given cell and its second nearest cells.

It is known that the movements of ions are modified by tortuosity in the extracellular micro-environment of the brain tissue [39,40]. Tortuosity is taken into account by introducing a factor λ which is associated with lateral diffusion time constant τ_{ss} and τ'_{ss} [17,31]:

$$\frac{1}{\tau_{\mathrm{ss}}} = \frac{D_K}{(\lambda \times x)^2}; \quad \frac{1}{\tau'_{\mathrm{ss}}} = \frac{D_K}{(\lambda \times x')^2}, \tag{11}$$

where D_K is diffusion coefficient for K^+ and x and x' are described as a distance between the centers of two interstitial volumes. Thus,

$$\frac{\tau_{\mathrm{ss}}}{\tau'_{\mathrm{ss}}} = \frac{x^2}{x'^2}. \tag{12}$$

We obtain $\tau'_{\mathrm{ss}} = 3.3\tau_{\mathrm{ss}}$ by applying the method in the Appendices of Ref. [31].

The potassium coupling strength κ is defined as

$$\kappa = \log_{10}(1000\,\mathrm{ms}/\tau_{\mathrm{ss}} + 1). \tag{13}$$

Thus,

$$\tau_{\mathrm{ss}} = \frac{1000\,\mathrm{ms}}{10^\kappa - 1}. \tag{14}$$

The above two equations describe the relation potassium coupling strength and potassium diffusion constant τ_{ss}. This rela-

tion is consistent with the fact that a faster movement of potassium ions provides a stronger mutual interaction between cells.

C. Electrical coupling

Electrical coupling is modeled by adding a coupling current to Eq. (1) for the soma of each cell. Then the dynamics of the somatic membrane potential of cell i becomes

$$C_s \frac{dV_s^i}{dt} = -\left(I_{Na}^i + I_K^i + I_{sLeak}^i + I_{pump}^i + I_{sd}^i + I_{gap}^i\right) + I_{stim}^i,$$
$$I_{gap}^i = \sum_j g_{gap}\left(V_s^i - V_s^j\right), \quad (15)$$

where the sum is over the nearest cells of cell i and g_{gap} is the electrical coupling conductance between the cells i and j. There is little direct experimental evidence for gap junctions on CA1 pyramidal neurons. In the CA1 region, neurons are densely packed and it has been suggested somatic contacts can be an option for pyramid-pyramid electrical junctions [35]. Thus, the cells are electrically coupled through somatic gap junctions in our model.

III. RESULTS

A. The presence and absence of potassium coupling

We perform simulations with and without potassium lateral diffusion to study the role of potassium diffusion in the

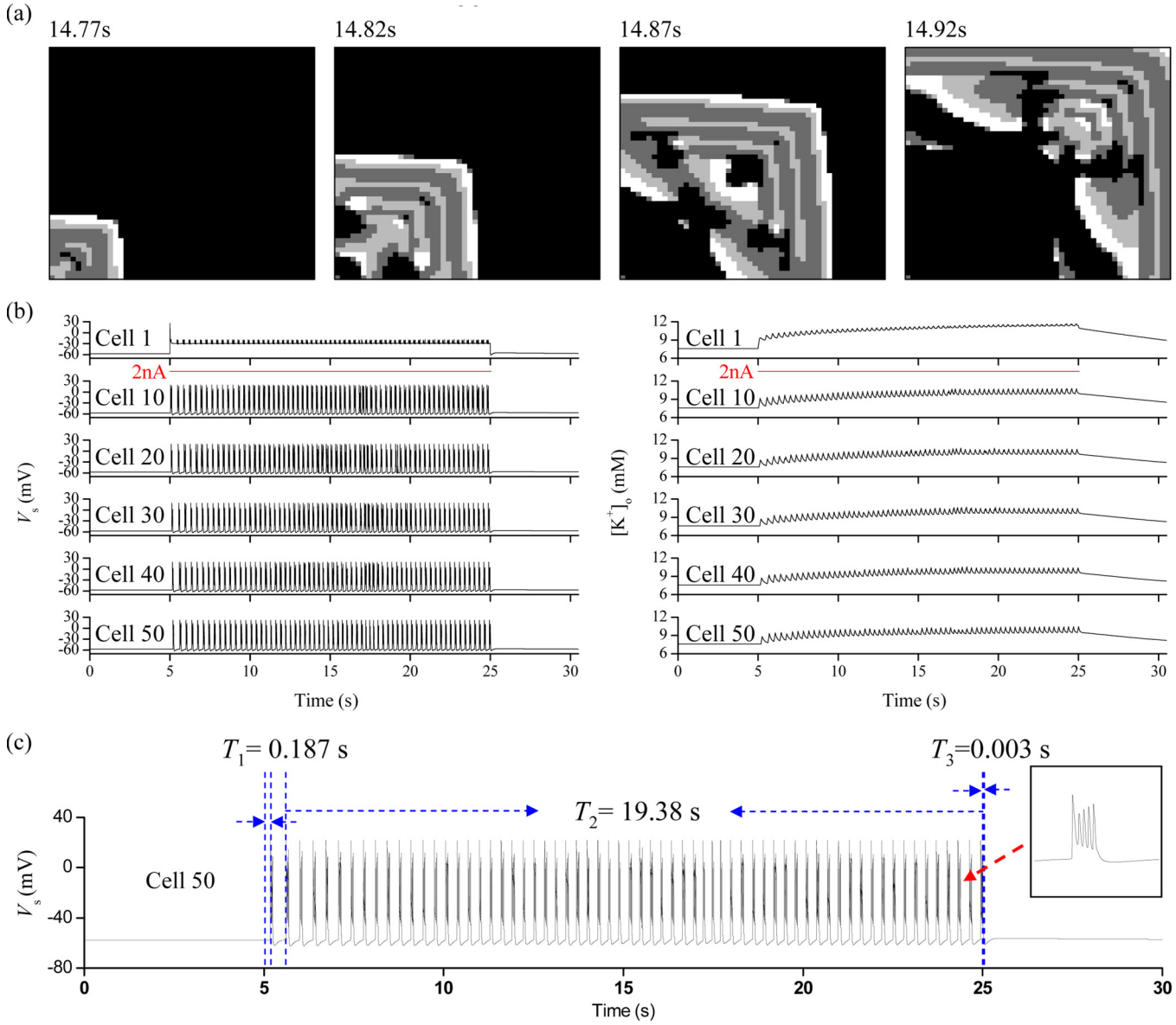

FIG. 2. (Color online) Network oscillations for neurons which are coupled through gap junctions ($g_{gap} = 0.55$ mS/cm^2) and potassium lateral diffusion ($\kappa = 1.5$). A current pulse (20 s, 2 nA) applied to cell 1 is used to induce action potentials. (a) Snapshots of voltage waves in the cell network; (b) time series of V_s and $[K^+]_o$ of cell 1, 10, 20, 30, 40, and 50, respectively; (c) the latency of the first spike after the application of the stimulation T_1, the duration of network oscillations T_2, and the remaining activity duration after the end of stimulation T_3. A five-spike burst is depicted in the enlarged drawing in the right of (c). In the gray patterns in (a), the black dots represent $V_s = -60$ mV and white dots 30 mV.

generation of spiking activity in an electrically coupled cell network. We start with the neuron network modeling with both the electrical connections and potassium diffusion among nearby neurons. Neurons are arranged as in Fig. 1(d) with $g_{\text{gap}} = 0.55$ mS/cm^2 and $\kappa = 1.5$. The choice of κ here leads to the result of $\tau_{\text{ss}} \approx 32$ ms, which is consistent with the values given in Ref. [31], which are considered to be physiologically reasonable. The background state is silent without any stimulation. Network oscillations are observed when a DC pulse with an amplitude of 2 nA and a duration of 20 s is applied to cell 1.

Figure 2(a) shows the snapshots of action potential waves in the network with potassium coupling at $\kappa = 1.5$, which are symmetric due to the symmetry structure of the model. Dots in lighter color indicate cells being more depolarized, and black areas indicate that the cells there are at their silent states. Figure 2(b) plots the trajectories of V_s and $[\text{K}^+]_{\text{o}}$ in cells 1, 10, 20, 30, 40, and 50 [see Fig. 1(d) for cell positions], respectively. As shown in Fig. 2(b), the electrical stimulation causes cell 1 to generate a burst and then enter a state known as depolarization block [41]. Through gap junctions and potassium diffusion, series of action potentials are generated in all the cells of the network following the onset of the stimulus.

During the electrical stimulation, cell 1 is depolarized to be depolarization block, which provides a stable source of potassium ions to its nearby cells directly and farther away cells indirectly through potassium diffusion. The increase in the potassium concentration in the interstitial spaces of these cells makes them easier to get excited with action potentials. Thus, other cells in this network have two input signals from the stimulated cell: a depolarized electrical signal through electrical junctions and a potassium signal through ion diffusion. As a result, action potential waves [Fig. 2(a)] almost start at the moment when the stimulus is applied.

Figure 2(a) depicts the spread of a burst in the network as a wave. The burst starts from cell 1 and then affects its nearby cells. Later these cells turn quiescent but cells further away from cell 1 become turned on. This process repeats itself until cell 50 is lighted. The time of the occurrence of each burst in one cell is generally dependent on the distance of that cell from the stimulated cell. Once started, the oscillation bursts in this locally coupled network with gap junctions propagate with a much larger velocity than other signals among cells (e.g., intracellular calcium waves in astrocytes) [42,43]. After the stimulus, which is turned on at $t = 5$ s, terminates at $t = 25$ s, potassium regulating mechanisms start to overpower the ionic currents, and then finally the interstitial potassium fails to maintain the oscillations in the network.

However, when the same simulation is repeated without potassium lateral diffusion ($\kappa = 0$), the results are different (Fig. 3). With DC stimulation, cell 1 is in depolarization block after the first burst. Thus there is a large amount of potassium ions flowing into the interstitial space. But the increase of $[\text{K}^+]_{\text{o}}$ of cell 1 could not create diffusion of K^+ to neighboring regions when potassium diffusion coupling is removed. Instead the increasing potassium accumulation makes cell 1 more positive. Meanwhile, through gap junctions, cell 1 produces a depolarizing signal for nearby cells. When this signal is strong enough, i.e., about 10 s after DC stimulation is on, cells in the network start oscillating. The bursts are firstly generated in cell 1 and then in nearby cells. They then proceed to diffuse outward to other cells and finally to cell 50. To give an example, we plot in Fig. 3(a) snapshots of the spreading of a burst in the network.

After the stimulus is removed, the potassium concentrations gradually decrease. However, the periodic oscillations of these neurons elevate $[\text{K}^+]_{\text{o}}$ in the network so significantly that it is able to maintain network oscillations for several seconds even after stimulus stops at 25 s.

To examine the activity generated in the cell network, we introduce the concept of the latency of the first spike after the application of the stimulation (T_1), the duration of network oscillations (T_2), and the remaining activity duration after the end of stimulation (T_3). We use the voltage time series of cell 50 to obtain $T_{1,2,3}$ according to $T_1 = t_1 - t_{\text{start}}$, $T_2 = t_3 - t_2$, and $T_3 = t_3 - t_{\text{end}}$, in which t_{start} is the starting time that the DC stimulus is applied to cell 1, t_{end} the end time of the DC stimulus, t_1 the beginning time of the first spike, t_2 the beginning time of the second burst, and t_3 the end time of the last spike.

With both the couplings through gap junctions and potassium diffusion ($g_{\text{gap}} = 0.55$ mS/cm^2, $\kappa = 1.5$), the neuronal oscillations continue for $T_2 = 19.38$ s and almost immediately disappear at the stimulus termination [Fig. 2(c)]. The scenario is different as the potassium coupling is removed. As indicated in Fig. 3(c), the periodic oscillations last for $T_2 = 12.246$ s, and the remaining activity duration after stimulus is $T_3 = 2.176$ s. As to the first spike of cell 50, it is generated in the electrically coupled neurons at $T_1 = 0.187$ s after the application of the stimulus regardless of the existence of the potassium diffusion. The reason that the presence of potassium lateral diffusion does not affect the latency of the first spike is that the first spike is generated before the evident potassium accumulation. Therefore, the speed of this first burst depends only upon the gap-junction strength, unaffected by the potassium coupling strength.

B. Effects of potassium coupling and gap junction on the activity

As shown in the last subsection, depolarization block following an initial burst is elicited in the stimulated cell by a DC current. This constantly provides its neighboring neurons with electrical currents through gap junctions and potassium inflow through diffusion. These two flows then cover the whole network, along with the action potential waves. It is shown that the involvement of potassium lateral diffusion results in a longer duration of the action potential waves. We now investigate how the stimulus-induced activity responds to the variation of potassium coupling strength and gap junction conductance. Figure 4 shows the relationship of $T_{1,2,3}$ to κ and g_{gap}.

Compared to the well-known electrical coupling, we are more interested in the role played by the potassium diffusion in a neuron network, which is much less understood but suggested to be involved in some important network activities. As mentioned previously in Eq. (11), potassium lateral diffusion strength depends on tortuosity and the distance between two interstitial volumes. Modifying κ can be understood as a change in these basic quantities. Although the value of κ

chosen for Fig. 2 is considered physiologically reasonable, a change in the structure of the tissue can lead to the variation of these basic quantities. It is valuable to know what results would be caused by such a change.

We can see from Fig. 4(a) that the latency of the first spike T_1 is almost independent of potassium coupling κ except for small values of g_{gap}. For $g_{gap} = 0.275$ mS/cm^2, the effect of electrical coupling to the network becomes so weak that increasing potassium coupling strength can slightly reduce T_1. On the contrary, the latency of the first spike at cell 50 decreases exponentially with increasing gap-junction conductance, indicating the increase of the spreading speed of each burst in the network.

The duration of network oscillations T_2 is shown in Fig. 4(b). We notice a plateau with large g_{gap} values where T_2 is less sensitive to κ. Considering that the depolarization block state of the stimulated cell provides a steady DC input to the four neighboring neurons, the strong gap junction alone is enough not only to evolve the action potentials in these four neighboring neurons, but also to spread the action potential waves in the network.

For $0.3 < g_{gap} < 0.6$ mS/cm^2, the correlation curves between coupling strength κ and oscillation duration T_2 are bell-like shapes, which are a surprising result at first glance. Without potassium diffusion, such gap-junction coupling alone can only generate a slow spreading wave of action potential in the network, giving a small oscillation duration T_2. As the potassium diffusion coupling strength increases, extracellular potassium ions can move easily to neighboring cells. The elevated $[K^+]_o$ of cell 1 will first diffuse to the nearby

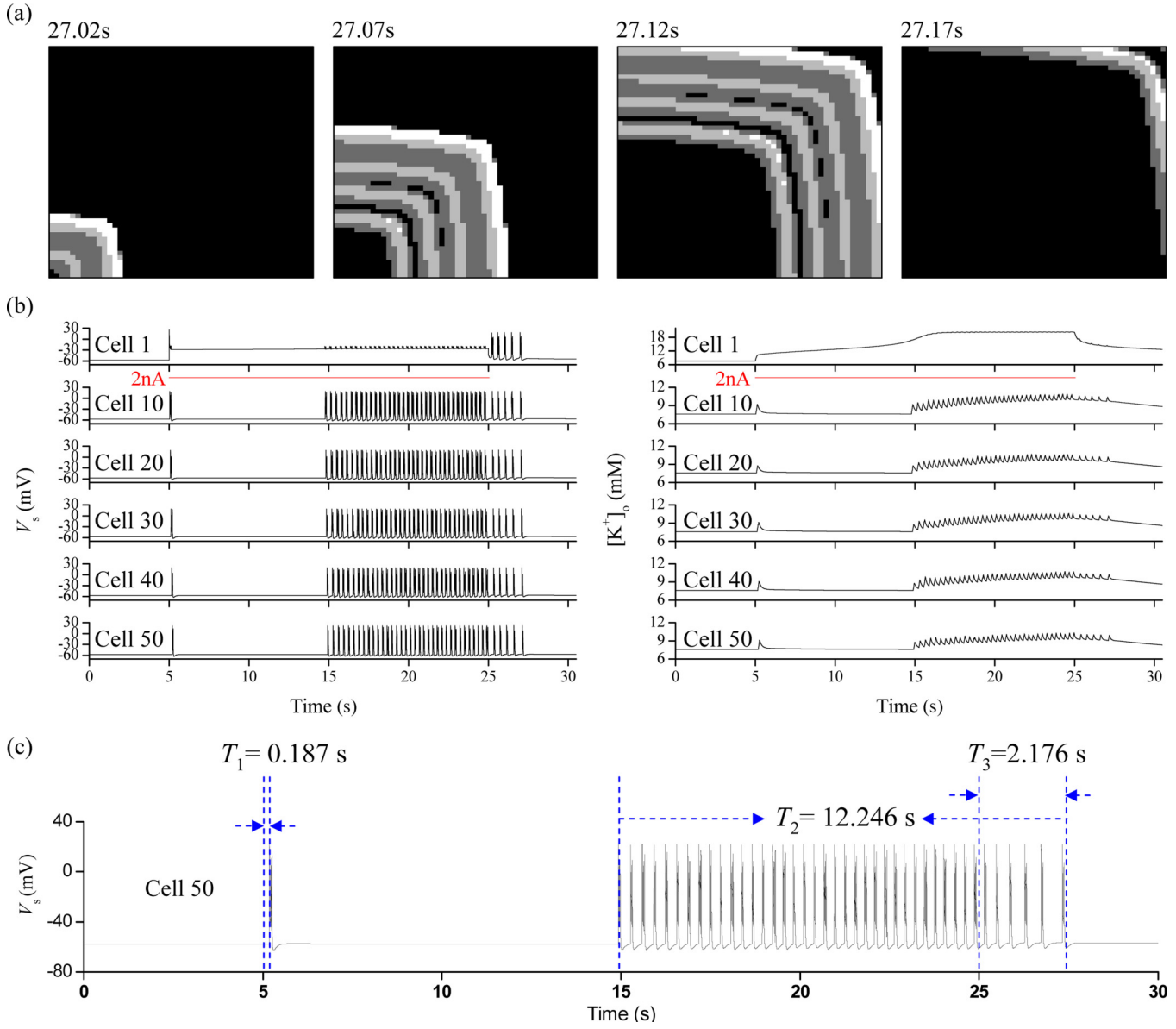

FIG. 3. (Color online) Network oscillations for neurons which are coupled only through gap junctions ($g_{gap} = 0.55$ mS/cm^2, $\kappa = 0$). The same current pulse (20 s, 2 nA) is applied to the cell 1. (a) Snapshots of voltage waves in the cell network; (b) time series of V_s and $[K^+]_o$ of cell 1, 10, 20, 30, 40, and 50, respectively; (c) the latency of the first spike T_1, the duration of network oscillations T_2, and the remaining activity duration T_3. In the gray patterns in (a), the black dots represent $V_s = -60$ mV and white dots 30 mV.

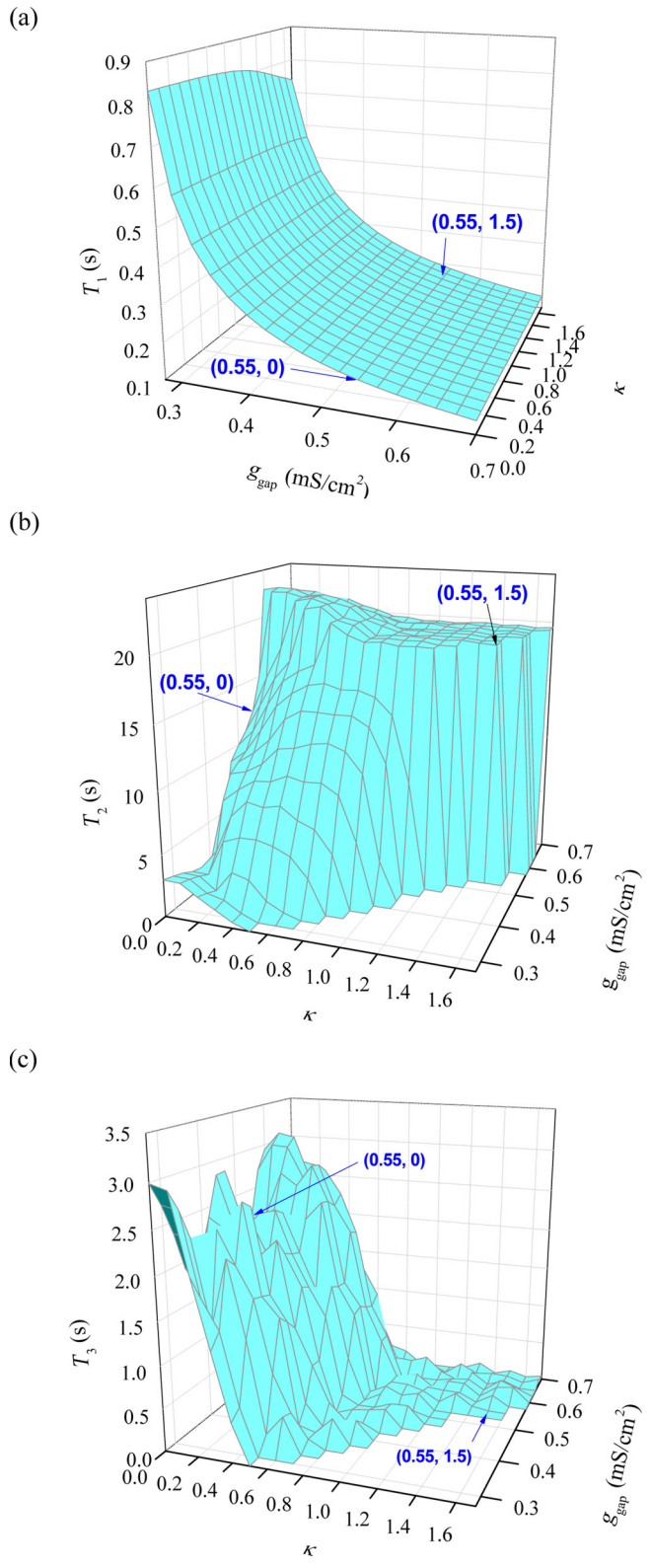

FIG. 4. (Color online) Two-dimensional distribution of the latency of the first spike T_1 (a), the length of network oscillations T_2 (b), and the length of activity after the end of stimulation T_3 (c) as a function of potassium diffusive coupling strength κ and gap-junction strength g_{gap}. The first plot is shown in a different orientation only to show the whole view.

resting neurons, making these neurons easily depolarized. These nearby firing neurons will then release more K^+ ions into their interstitial space, which will also diffuse into their nearby resting neurons to evolve action potentials. As a result, the potassium lateral diffusion at an intermediate range of κ around 0.5 can easily generate action potential waves in the network, producing a long oscillation duration T_2. When the potassium lateral diffusion strength is high, the potassium ions will spread rapidly into the whole network to approach the equilibrium state. As a result, even for those resting neurons which are near to the spiking ones, they could not accumulate enough $[K^+]_o$ to evoke an action potential. Thus, at large κ we have $T_2 = 0$, showing no network oscillations. This discussion indicates that, at weak gap-junction coupling, an optimal potassium diffusion can drive and accumulate enough $[K^+]_o$ from the spiking neurons to its nearby resting neurons, and then easily evoke action potentials in these nearby cells, generating activity waves in the network.

Figure 4(b) also shows that abrupt changes in the activity duration appear under the conditions of strong potassium lateral diffusion compared to relatively smooth changes for weak potassium lateral diffusion. In particular, we see that an activity of nearly $T_2 = 20$ s is observed for $g_{gap} = 0.55$ mS/cm^2 and $\kappa = 1.5$ but completely abolished for $g_{gap} = 0.525$ mS/cm^2 and the same value of κ. Hence, the neuron network responses to the electrical stimulus in an all-or-none fashion at strong potassium lateral diffusion.

It is notable that the remaining activity duration T_3 fluctuates in the order of nearly 0.5 s by a small variance in κ or g_{gap}, which causes obvious perturbations in the two-dimensional surface in Fig. 4(c). This is because the interburst interval can be as large as 0.5 s and the largest value for T_3 is only about 3 s. Despite the stochastic-like fluctuations, Fig. 4(c) shows that the remaining activity duration after the stimulus is relatively insensitive to g_{gap}, while it decreases with increasing potassium diffusion intensity. The reason is that during this period the accumulated interstitial potassium concentration in cell 1 is a main factor to drive the neuron network to oscillate. The process of restoring the equilibrium state would be accelerated, if the potassium lateral diffusion ability is increased which thereby reduces more the interstitial potassium accumulation in the stimulated cell.

C. Locally random topology for gap junctions

With a deterministic topology for gap-junction coupling between nearest neighbor cells, we have revealed that potassium diffusion strength has a nontrivial effect on the network response. But in more realistic situations, gap-junction connections are not regular. To verify that our conclusion can still persist in a more realistic network, a smaller network of 400 cells has been used with the same structure of the network in Fig. 1(d). The neurons are placed in the same plane with 20 rows of cells and 20 columns of cells. Potassium diffuses in the same way between the interstitial spaces of neighboring cells as in Fig. 1(b), but the strategy for the electrical coupling is changed. It is biologically realistic for

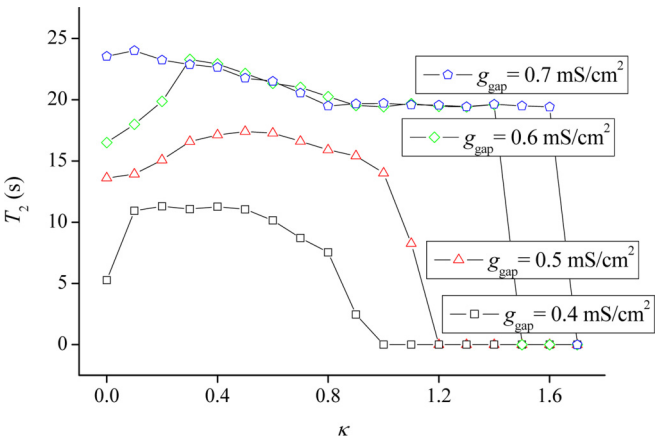

FIG. 5. (Color online) The length of activity T_2 as a function of potassium diffusive coupling strength κ for $g_{gap} =$ 0.4, 0.5, 0.6, and 0.7 mS/cm^2. The network used here is similar to the one described in Fig. 1 except that it is a structure of 20 × 20 neurons and with a random gap-junction topology.

every cell to be connected randomly by gap junctions with its most neighboring cells and second most neighboring cells. We consider the situation where each cell has four random gap-junction connections with its most neighboring cells and second most neighboring cells, which leads to the same number of connections per neuron with the previous regular network.

Figure 5 describes the results for a random topology for $g_{gap} = 0.4$, 0.5, 0.6, and 0.7 mS/cm^2. For $g_{gap} = 0.4$ mS/cm^2 and $g_{gap} = 0.5$ mS/cm^2, the dependence of T_2 on κ shows a bell-shaped curve. For $g_{gap} = 0.6$ mS/cm^2 and $g_{gap} =$ 0.7 mS/cm^2, the value of T_2 seems relatively more stable for most κ values, and the change in T_2 exhibits an abrupt drop with the increase of κ. Therefore, the conclusions that persist for a deterministic gap-junction topology are still correct for a locally random topology for the gap junction connections.

IV. CONCLUSION

A stimulus can induce action potentials in a single neuron accompanied by an increase in the interstitial potassium concentration, which in turn further depolarizes that neuron. When neurons are coupled electrically and with potassium diffusion and one of them is stimulated, the firing activity can be generated in the entire network, which is accompanied by the diffusion of potassium ions from the stimulated cell to other cells. In this study, we find that potassium diffusion strength has a strong influence on the network outcomes. In addition, our results are consistent with the popular view that gap junctions provide a favorable condition for electrical oscillations. However, our attention is more drawn towards the nontrivial effects of the potassium coupling strength on network dynamics.

As the values of potassium diffusion strength and electrical coupling strength are varied gradually, the network oscillations induced by electrical stimulus show different patterns. The onset time of the first spike exponentially depends on the electrical coupling strength. The remaining activity after stimulation is caused by the potassium accumulation in the stimulated cell, the reduction of which by increasing potassium lateral diffusion strength would thus decrease the length of this activity. In particular, we show that the relations of the activity duration to potassium coupling strength can be nonmonotonic. The reason is that potassium coupling exerts its influence over the network through two pathways. An increment of potassium lateral diffusion strength leads to decreased interstitial potassium concentration in the stimulated cell but increased interstitial potassium concentration in other cells of the network. It is known that potassium accumulation around a neuron favors the depolarization of this neuron's membrane. Thus, the increase in potassium diffusion strength has two opposite impacts on the depolarization of the different neurons.

Although whether or not the role of potassium dynamics is a primary mechanism in the initiation of hippocampal seizures has been debated, potassium accumulation was suggested to account for the firing activity having an all-or-nothing manner [12,44]. In our simulation, we show that when potassium lateral diffusion and electrical coupling strength are strong, the oscillations in the neuron network can occur during the stimulus pulse or be deleted with a small increment in the potassium diffusion strength, exhibiting an all-or-none fashion.

A relatively strong current is injected to the stimulated neuron in the network and it exhibits depolarization block behavior following an initial burst. It has been suggested that the depolarization block would be typically observed in CA1 neuronal model with a strong stimulus, which could be physiologically reachable [41]. As indicated in Ref. [41], considering the average peak current with an excitatory synaptic input to be 13–25 pA [45], the background synaptic activity in the gamma range involving less than 3% of the total number of excitatory synaptic inputs converging on any given CA1 pyramidal neuron could easily generate an aggregate peak input current larger than 1 nA. As a result, in a large active network some cells are likely to enter the state of depolarization block at some time duration, acting as the stimulated neuron in our model, to generate action potential waves in the network, which puts our discussion biologically meaningful. The chemical synapses are inactive in our model and here we do not intend to incorporate chemical synapses into the network but to explain that the stimulus amplitude we adopt is similar to the current through chemical synapses and is a biologically reasonable value.

In our simulations, the stimulated neuron provides potassium ions for other neurons and intracellular spaces act as a source of potassium. It is assumed in this modeling that $[K^+]_{bath} = 7.6$ mM and $[K^+]_i = 140$ mM for the fixed potassium concentrations of the interstitial spaces and of the bath, respectively. The total intraneuronal volume is about twice the size of total extracellular volume [46]. Thus, the variation in the same amount of potassium ions leads to a larger change in $[K^+]_o$ than in $[K^+]_i$. However, possible artifact may be introduced by fixing intracellular potassium concentrations, especially in the situations of high potassium lateral diffusion strength. A more biologically realistic model with variable intracellular potassium concentrations will be considered in our future study.

The adopted CA1 neuron model consists of 16 compartments with 15 compartments for dendrites in order to simulate

the dendritic structure of the neuron. However, the dendrite structure plays little role in the network activities in our simulations, because dendrite compartments only incorporate passive channels and both potassium and electrical couplings only occur between soma compartments. We believe that a simplified CA1 model with only soma compartment will produce the similar results, although it would enrich our modeling to include active ionic channels on the dendrites and potassium diffusion among soma and dendrite compartments.

In conclusion, we show that the potassium lateral diffusion plays a nontrivial role on the oscillatory activity of an electrically coupled neuron network induced by a DC stimulus. The dependence of the duration of the firing activity on potassium lateral diffusion strength displays bell-like shapes at weak gap junction coupling. Thus, there is an optimal potassium diffusion strength, at which potassium accumulation is ideally distributed among the network neurons to best facilitate the generation and continuance of the spread of the spiking waves. An all-or-none firing activity is also found at strong gap junction coupling and strong potassium lateral diffusion, which may also be biologically relevant.

ACKNOWLEDGMENTS

We acknowledge support from the National Natural Science Funds for Distinguished Young Scholar of China under Grant No. 11125419, the National Natural Science Foundation of China under Grant No. 31370830, and the Fujian Province Funds for Leading Scientist in Universities. Computational support from the Key Laboratory for Chemical Biology of Fujian Province, Xiamen University, and Xiamen Super Computing Center is gratefully acknowledged.

[1] M. Müller and G. G. Somjen, J. Neurophysiol. **83**, 735 (2000).
[2] E. I. Ekinci, K. Y. Cheong, M. Dobson, E. Premaratne, S. Finch, R. J. MacIsaac, and G. Jerums, Diabet. Med. **27**, 1401 (2010).
[3] L. M. Resnick, M. Barbagallo, L. J. Dominguez, J. M. Veniero, J. P. Nicholson, and R. K. Gupta, Hypertension **38**, 709 (2001).
[4] A. Zaza, Europace **11**, 421 (2009).
[5] B. Frankenhaeuser and A. L. Hodgkin, J. Physiol. **131**, 341 (1956).
[6] E. C. Zuckermann and G. H. Glaser, Exp. Neurol. **20**, 87 (1968).
[7] G. Moddel, A. Gorji, and E. J. Speckmann, Brain Res. **959**, 135 (2003).
[8] U. Strauss, F. W. Zhou, J. Henning, A. Battefeld, A. Wree, R. KoehlIng, S. J. P. Haas, R. Benecke, A. Rolfs, and U. Gimsa, J. Neurophysiol. **99**, 2902 (2008).
[9] W. R. Anderson, J. E. Franck, W. L. Stahl, and A. A. Maki, Epilepsy Res. **17**, 221 (1994).
[10] S. Gabriel, A. Eilers, A. Kivi, R. Kovacs, K. Schulze, T. N. Lehmann, and U. Heinemann, Neurosci. Lett. **242**, 9 (1998).
[11] J. Lian, M. Bikson, J. W. Shuai, and D. M. Durand, J. Physiol. **537**, 191 (2001).
[12] Y. Yaari, A. Konnerth, and U. Heinemann, J. Neurophysiol. **56**, 424 (1986).
[13] F. Amzica, M. Massimini, and A. Manfridi, J. Neurosci. **22**, 1042 (2002).
[14] U. Heinemann, H. D. Lux, and M. J. Gutnick, Exp. Brain Res. **27**, 237 (1977).
[15] G. G. Somjen, P. G. Aitken, J. L. Giacchino, and J. O. McNamara, J. Neurophysiol. **53**, 1079 (1985).
[16] G. Florence, T. Pereira, and J. Kurths, Commun. Nonlinear Sci. Numer. Simulat. **17**, 4700 (2012).
[17] M. Bazhenov, I. Timofeev, M. Steriade, and T. J. Sejnowski, J. Neurophysiol. **92**, 1116 (2004).
[18] X. X. Wu and J. W. Shuai, Phys. Rev. E **85**, 061911 (2012).
[19] F. Frohlich and M. Bazhenov, Phys. Rev. E **74**, 031922 (2006).
[20] H. Kager, W. J. Wadman, and G. G. Somjen, J. Neurophysiol. **84**, 495 (2000).
[21] J. R. Cressman, G. Ullah, J. Ziburkus, S. J. Schiff, and E. Barreto, J. Comput. Neurosci. **26**, 159 (2009).
[22] E. Barreto and J. R. Cressman, J. Biol. Phys. **37**, 361 (2011).
[23] T. Lau, G. J. Gage, J. D. Berke, and M. Zochowski, Phys. Biol. **7**, 016015 (2010).
[24] S. Nadkarni and P. Jung, Phys. Biol. **4**, 1 (2007).
[25] Y. Loewenstein, Y. Yarom, and H. Sompolinsky, Proc. Natl. Acad. Sci. USA **98**, 8095 (2001).
[26] T. Nowotny and M. I. Rabinovich, Phys. Rev. Lett. **98**, 128106 (2007).
[27] D. O. C. Santos, A. M. Rodrigues, A. C. G. de Almeida, and R. Dickman, Phys. Biol. **6**, 046019 (2009).
[28] C. L. Stokes and J. Rinzel, Biophys. J. **65**, 597 (1993).
[29] G. Ullah, John R. Cressman, Jr., Ernest Barreto, and Steven J. Schiff, J. Comput. Neurosci. **26**, 171 (2009).
[30] D. M. Durand, E. H. Park, and A. L. Jensen, Philos. Trans. R. Soc. B **365**, 2347 (2010).
[31] E. H. Park and D. M. Durand, J. Theor. Biol. **238**, 666 (2006).
[32] G. Florence, M. A. Dahlem, A. C. G. Almeida, J. W. M. Bassani, and J. Kurths, J. Theor. Biol. **258**, 219 (2009).
[33] E. H. Park, Z. Feng, and D. M. Durand, Biophys. J. **95**, 1126 (2008).
[34] A. Mercer, A. P. Bannister, and A. M. Thomson, Brain Cell Biol. **35**, 13 (2006).
[35] A. Mercer, Brain Res. **1487**, 192 (2012).
[36] A. Draguhn, R. D. Traub, D. Schmitz, and J. G. R. Jefferys, Nature (London) **394**, 189 (1998).
[37] J. E. Rash, H. S. Duffy, F. E. Dudek, B. L. Bilhartz, L. R. Whalen, and T. Yasumura, J. Comp. Neurol. **388**, 265 (1997).
[38] J. W. Shuai, M. Bikson, P. J. Hahn, J. Lian, and D. M. Durand, Biophys. J. **84**, 2099 (2003).
[39] C. J. Mcbain, S. F. Traynelis, and R. Dingledine, Science **249**, 674 (1990).
[40] C. Nicholson and J. M. Phillips, J. Physiol. **321**, 225 (1981).
[41] D. Bianchi, A. Marasco, A. Limongiello, C. Marchetti, H. Marie, B. Tirozzi, and M. Migliore, J. Comput. Neurosci. **33**, 207 (2012).
[42] A. Strahonja-Packard and M. J. Sanderson, Glia **28**, 97 (1999).
[43] F. Wei and J. W. Shuai, Phys. Biol. **8**, 026009 (2011).
[44] E. R. C. Sanabria, H. L. Su, and Y. Yaari, J. Physiol. **532**, 205 (2001).
[45] B. K. Andrásfalvy and J. C. Magee, J. Neurosci. **21**, 9151 (2001).
[46] K. C. Chen and C. Nicholson, Biophys. J. **78**, 2776 (2000).